

Optical, electrical and antimicrobial studies of chemically synthesized graphite oxide and reduced graphene oxide

Alpana Thakur^{1*}, Sunil Kumar², Manjula Sharma³, V. S. Rangra¹

¹Department of Physics, Himachal Pradesh University, Shimla 171005, Himachal Pradesh, India

²Department of Chemistry, Sri Sai University, Palampur 176081, Himachal Pradesh, India

³Department of Physics, National Institute of Technology, Hamirpur 176081, Himachal Pradesh, India

*Corresponding author. E-mail: alpanarangoli@gmail.com

Received: 04 April 2016, Revised: 16 June 2015 and Accepted: 22 June 2016

ABSTRACT

Graphite oxide (GO) and reduced graphene oxide (RGO) have been synthesized using chemical methods. Prepared graphite oxide and reduced graphene oxide were characterized by X-ray diffraction (XRD), scanning electron microscopy (SEM), Fourier transform infrared spectroscopy (FTIR) and Raman spectroscopy. XRD patterns, Raman spectra and FTIR spectroscopy confirms significant structural changes while reducing GO to RGO. The obtained products were further analyzed for their optical and electrical properties using UV-Vis spectroscopy, photoluminescence spectroscopy and four-point probe. RGO has shown excellent electrical conductivity of 1.363×10^4 S/m. The bactericidal action of prepared GO and RGO was also studied against *Escherichia coli* and *Staphylococcus aureus* bacteria. Copyright © 2016 VBRI Press.

Keywords: Raman spectroscopy; reduced graphene oxide; chemical synthesis; electrical conductivity; optical properties.

Introduction

Graphene is the hottest member of carbon allotropic family since its discovery in 2004. It is thinnest material ever synthesized and has extensive potential for a wide range of applications due to its admirable electrical, optical and mechanical properties. Graphene is almost transparent with more than 98% optical transmittance [1]. It has exceptionally high Young's modulus of about 1.0 TPa but still it is quite elastic [2].

Since graphene is excellent conductor with thermal conductivity of about $5000 \text{ W m}^{-1} \text{ K}^{-1}$ and have highest reported intrinsic mobility of $200,000 \text{ cm}^2 \text{ V}^{-1} \text{ s}^{-1}$ [3-4]. Thus graphene has boosted the field of nanoelectronics photo-electronic and energy storage [5-6]. Graphene sheets can also be utilised for enzyme immobilisation leading its use in programmable bioelectronics [7]. Beside these graphene is also used for biomedical applications such as in chemical and biochemical sensors [8]. Graphene possess high degree of antimicrobial properties thus can be used for developing newer antibiotics and strengthening the existing ones [9-10].

Due to the broad spectrum of properties many attempts have been made to produce these carbon sheets. The first and the most common method of production was mechanical exfoliation in which a scotch tape was used to exfoliate the sheets from graphite [11]. The method yield was very low so newer methods have been developed includes liquid-phase exfoliation, chemical vapour deposition (CVD), epitaxial growth, ion implantation and chemical oxidation of graphite following reduction of exfoliated graphite oxide sheets

[12-14]. Out of these the chemical method is the widely adopted process for the fabrication of graphene sheets due to its low cost and potential for large-scale industrial production.

In chemical method firstly graphite oxide (GO) is synthesized under vigorous conditions and then it is reduced to produce graphene (RGO) [15]. The oxygen containing functionalities in GO alters the van der Waals forces between the layers leading increased interlayer spacing and imparting hydrophilic nature to it. These hydrophilic layers can easily be exfoliated using ultrasonication in aqueous phase. Reduction with a suitable reducing agent is widely adopted method to produce RGO sheets from GO and to revive conjugated structure [16]. The choice of reducing agent affects the quality as well as yield of RGO and hydrazine hydrate is widely used for this reduction [17].

In the present work, GO and RGO have been synthesized via chemical method and the effect of chemical reduction has been studied by measuring electrical conductivity and optical parameters of RGO and GO. The effect of GO and RGO on bacteria *Escherichia coli* and *Staphylococcus aureus* have also been studied.

Experimental

Materials

Graphite flakes natural (-10 mesh, 99% metal basis) was obtained from Alpha Aesar. Potassium permanganate (KMnO_4), sulphuric acid (H_2SO_4), hydrogen peroxide (H_2O_2), hydrochloric acid (HCl) and hydrazine hydrate (N_2H_4) were supplied by Merck India. All the chemicals

were of analytical grade and were used without any purification. Water used in the synthesis was of high purity with specific conductance in the range of 0.1×10^{-6} to 1.0×10^{-6} S cm^{-1} and was prepared after series of distillation [18, 19]. Pure cultures of pathogenic bacteria (*E.coli.* and *S.aureus*) were procured from Indira Gandhi Medical College, Department of Microbiology, Shimla, India and were maintained on nutrient medium.

Synthesis of graphite oxide (GO)

Natural graphite flakes were used as the precursor in the modified Hummer's method for the synthesis of graphite oxide. Graphite flakes (3 g) were added into sulphuric acid (20 ml) and the mixture was sonicated for 2 h to produce a fine dispersion. The reaction mixture was heated at 90°C for 6 h with continuous stirring. The mixture was then poured into ice cold sulphuric acid (150 ml) kept under continuous stirring and potassium permanganate (15 g) was added slowly with extra care to keep mixture temperature below 10°C. The mixture was stirred continuously for 2 h or till it turns into thick solution. The solution was then diluted using distilled water. Hydrogen peroxide was added slowly into the diluted mixture and it was kept undisturbed for 24 h. The upper supernatant was separated, centrifuged and the obtained product was washed repeatedly with 30% HCl. Subsequently, the product was washed with distilled water three times to remove any acid and the wet material was then dried in an oven. The dried material was termed as graphite oxide (GO).

Synthesis of reduced graphene oxide (RGO)

RGO has been prepared by the reduction of graphite oxide using hydrazine hydrate as reducing agent. In typical procedure, graphite oxide powder (100 mg) was taken into a flask containing distilled water (100 ml) producing inhomogeneous dispersion. This dispersion was then treated with ultrasonic frequency in an ultrasonicator producing homogeneous solution containing large number of exfoliated single and multi-layers of graphene oxide. These exfoliated layers were freed from oxygen functionalities by drop-wise addition of hydrazine hydrate (1ml). The mixture was then heated in water bath under a water-cooled condenser for 24 hrs at 90°C for complete reduction. Reduced GO was separated via filtration and washed with copious amount of water. The wet powder was dried in oven at 80°C and labelled as reduced graphene oxide powder (RGO).

Instrumentation

The infrared spectra were recorded in the range 4000-500 cm^{-1} with Alpha Bruker model using powder sample. The powder X-ray diffractions (XRD) were recorded on a Panalytical 3050/60 Xpert-PRO using Cu K_{α} radiation. Raman spectroscopy in the range 3500-1000 cm^{-1} was done using Reinshaw *in via* Raman microscope. Scanning electron microscope (SEM) images were captured on a FEI Quanta FEG 450. UV spectra were recorded using Shimadzu/UV-2600 UV-Visible spectrophotometer whereas PL-spectrophotometer FLS980-S2S2-s was used for PL spectra. For electrical conductivity measurements

GO and RGO were pressed into 13×1 mm cylindrical shaped samples. A four point probe resistance tester attached with Keithley Sourcemeter 6221 and Nanovoltmeter 2182A were used for electrical conductivity measurements of the GO and RGO samples.

Antibacterial studies

Antibacterial activities of GO and RGO were tested against *Escherichia coli* and *Staphylococcus aureus* in distilled water as well as in acetone and commercial drug streptomycin was used for comparison. Nutrient agar medium was used for the growth of microorganisms and screening of the samples was done using agar well diffusion method. The medium was autoclaved at 121.6°C for 30 minutes and the plates were kept overnight at room temperature to check for any contamination to appear. Bacteria were grown in nutrient broth for 24 hours and 100 μ l of bacterial suspension were spread on each nutrient agar plates [20]. Agar wells of 8mm diameter were prepared in each petri-plate with the help of sterilized stainless steel cork borer. The wells in each plate were loaded with 10mg of every sample and commercial drug Streptomycin, which has been used for comparison.

Plates loaded with only solvent were treated as control (C). The plates were incubated at 37°C for 24 hours in incubation chamber. Experiment was performed in triplicates. Activity was determined by measuring the diameters (in mm) of inhibition zone of bacterial colonies of treatment and control sets in mutually perpendicular direction. Growth inhibition was compared with the drug Streptomycin.

Results and discussions

Surface chemistry

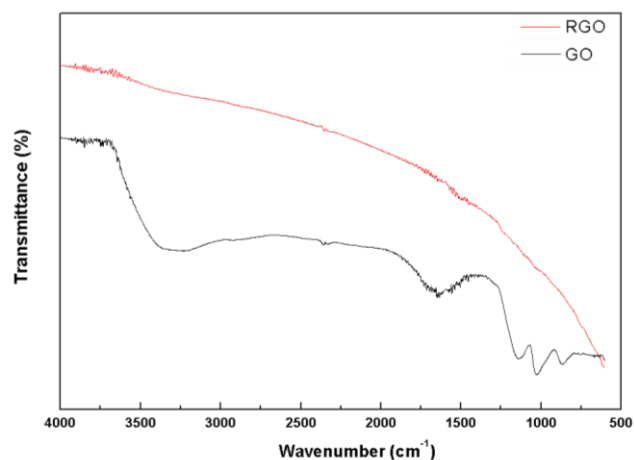


Fig. 1. FTIR spectra of RGO and GO.

Fourier transform infrared spectroscopy

FTIR spectroscopy has been employed to depict various moieties and functionalities present in GO and effect of reduction on these functional groups. The FTIR spectra of GO (Fig. 1) shows absorption bands confirming the presence of oxidizing groups. The broad peak around 2800-3300 cm^{-1} was due to O-H stretching of absorbed

water on the surface of GO [21]. The skeletal vibrations of aromatic C=C domains were observed near 1600 cm^{-1} [22]. The alkoxy C-O vibrations were spotted around 1147 cm^{-1} and in-plane C-H stretching vibrations were noticed at 1031 cm^{-1} [23]. In the spectra of RGO (Fig. 1), all peaks corresponding to oxygen functional groups were diminished showing no sharp peaks confirming efficient reduction of GO.

Structural properties

X-ray diffraction

The structure of graphite, GO and RGO were investigated by XRD. The conversion of perfectly crystalline graphite to crystalline RGO involving GO as intermediate is clearly visible in Fig. 2. For pristine graphite, the XRD of graphite flakes was taken and an intensive peak at 26.61° was observed showing well organized layered structure of crystalline graphite with an interlayer spacing of 3.34 \AA [24]. XRD pattern of GO showed peak at 12.6° with an interlayer spacing of 6.98 \AA . The increase in the interlayer spacing indicates the oxidation of graphite with different functional groups positioned between graphitic layers [25]. The XRD pattern of RGO shows a broad peak corresponding to (002) graphitic lattice planes indicating reformation of network sp^2 carbon structures. The strong peak at 25.9272° for the (002) lattice plane corresponds to the interlayer spacing of 3.43 \AA showing highly crystalline nature of RGO [26]. The XRD data corresponding to (002) peak was fitted to Scherrer relation indicating monolayer or few-layered graphene sheets ~ 10 layers with in-plane crystallite size of 3.43 nm [27, 28]. The peak broadening of reduced graphene oxide signifies the smaller sheet size as compared to the graphite flakes and GO [29].

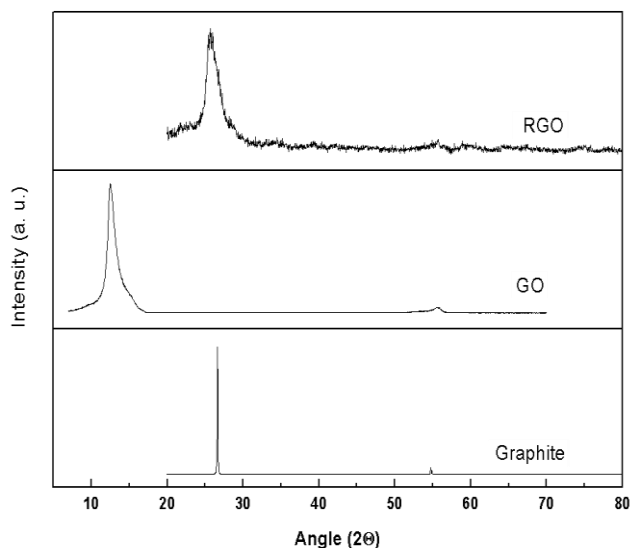


Fig. 2. XRD spectra of graphite, GO and RGO.

Raman Spectroscopy

Raman spectroscopy is useful non-destructive technique employed to study various carbon materials. Raman spectrum of graphite showed two peculiar peaks positioned at 1350 cm^{-1} and 1580 cm^{-1} designated as D band and G

band respectively [30]. The D band appears as a characteristic of the A_{1g} symmetry pointing up the existence of defects in the lattice and its intensity serves as a compute for short range disorders. Whereas the D band emerges due to first order scattering of sp^2 states and attributed to E_{2g} symmetry [31-32]. GO has less graphitic nature as it has lots of oxygen containing group and hence more sp^3 in character. Therefore Raman spectra showed only D and G bands and no second order signature that is 2D band.

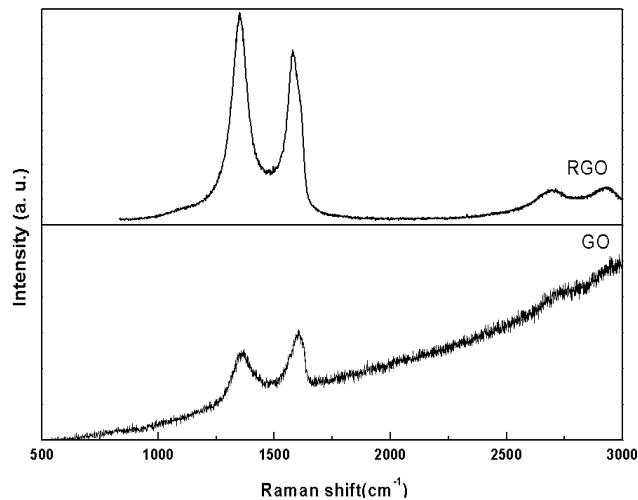


Fig. 3. Raman spectra of RGO and GO.

The Raman spectra of RGO showed more intense D band and two moderate bands at 2673.54 and 2916.42 cm^{-1} (Fig 3) corresponding to the second-order characteristics [33]. A Raman spectrum showed significant changes in going from GO to RGO (Fig. 3). The 'D' band for GO has been observed at 1360 cm^{-1} and the band shifted to 1353.49 cm^{-1} in RGO. A small blue shift from 1600 cm^{-1} to 1580.46 cm^{-1} in G band was also observed for RGO attributed to the recovery of network sp^2 character in RGO. The intensity ratio (I_G/I_D) has been associated with the in-plane crystallite size and was calculated using the equation [34]:

$$L_a = 4.4(I_G/I_D) \quad (1)$$

The calculated ratio I_G/I_D for RGO was 0.84 and for GO 1.14. The in-plane crystallite size was found to be 3.6 nm for RGO [35].

Scanning electron microscopy

The morphology and structure of RGO nanosheets were explored using SEM. SEM images of RGO (Fig. 4) showed paper-like structures with ripples and wrinkles on the surface; moreover, these ultrathin sheets appeared to be transparent. These features in the graphene lattice may be formed due to re-establishment of C sp^2 networks as a result of de-oxidation [36-37].

Optical analysis: UV-visible spectroscopy

UV-visible spectroscopy was used for the optical study of GO and RGO. UV-visible spectra for GO showed an absorption peak at 235 nm (Fig. 5) analogous to $\pi \rightarrow \pi^*$ transitions of aromatic C-C bands.

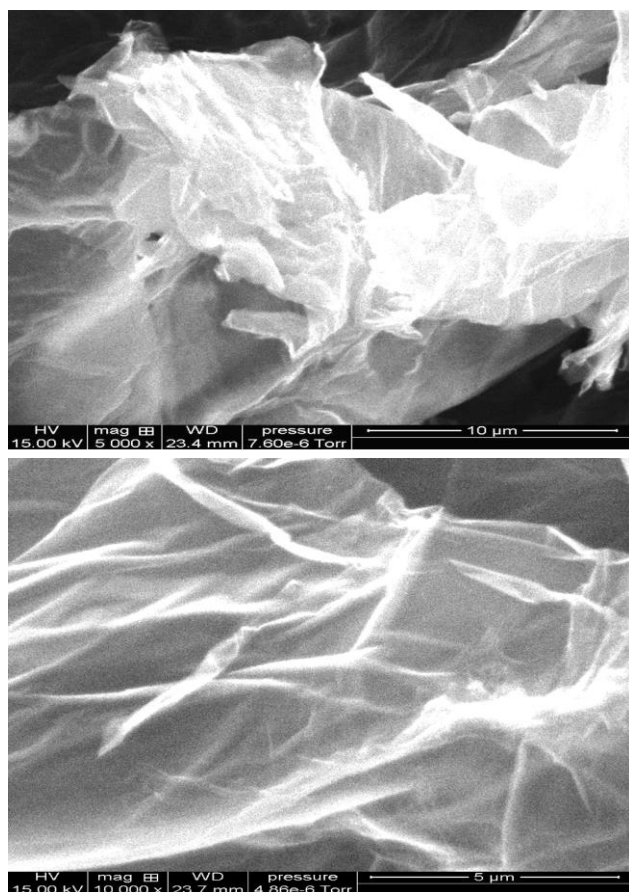


Fig. 4. SEM images of RGO.

After reduction the peak had shifted to 262 nm for RGO showing significant increase in conjugation attributed to decrease in oxygen containing functional groups and restoration of carbon-carbon double bonds (C=C) [38]. This confirms the successful reduction of graphene oxide [39].

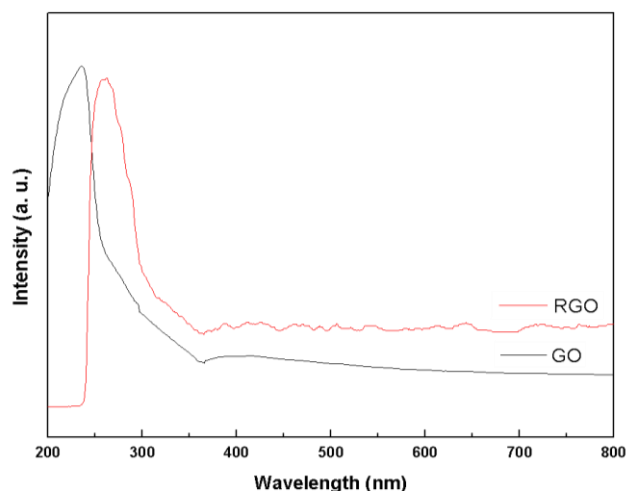


Fig. 5. UV-Vis spectra of RGO and GO.

Photoluminescence spectroscopy

Photoluminescence spectroscopy serves as a contactless, non-destructive technique to investigate the electronic

structure of materials. The intensity and spectral distribution of the emitted photoluminescence supplies important information related to recombination mechanisms, impurity levels, band gap and also helps in defect detections. The PL spectrum for GO and RGO dispersed in alcohol were obtained by the excitation wavelength 280nm. The PL of GO shows emission peak at 324 nm (Fig. 6) which results from the presence of π - π^* disorder-induced defect states [40]. The PL spectrum for RGO shows blue shift in the peak to 322 nm with low emission intensity indicating the decrease in the disordered states and increased number of small sp^2 clusters [41]. The lower PL intensity for RGO shows that the recombination rate for electron-hole pairs have been decreased as compared to that for the GO indicating the higher charge separation efficiency for RGO under light irradiation [42].

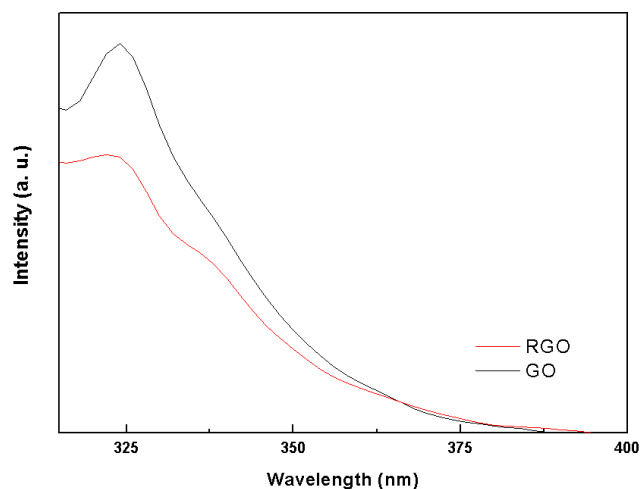


Fig. 6. PL of RGO and GO.

Electrical conductivity measurements

I-V Characteristics

The electrical conductivities of GO and RGO have been measured to verify the effect of chemical reduction in restoring the sp^2 graphitic networks. GO and RGO powders were pressed into 13×1 mm pellets using polyvinyl alcohol (PVA) as binder. Electrical conductivity of consolidated samples was measured at room temperature using four probe method. RGO exhibited excellent electrical conductivity of 1.363×10^4 S/m confirming the presence of sp^2 carbon network as in bulk graphite. Whereas GO exhibited lower electrical conductivity of 3.62×10^{-1} S/m due to the presence of oxygen groups. Conductivity of GO is attributed to incomplete oxidation of graphite flakes as GO was reported as insulating material [43-44].

Antibacterial studies

Both GO and RGO have shown good bactericidal effects both in acetone as well as in water as confirmed by the appearance of zone of inhibition in culture plates (Fig 7). The bactericidal effect of both GO and RGO was good in acetone as compared to distilled water. GO has shown good bactericidal effect in comparison to RGO but Streptomycin was better than both GO and RGO (Table 1).

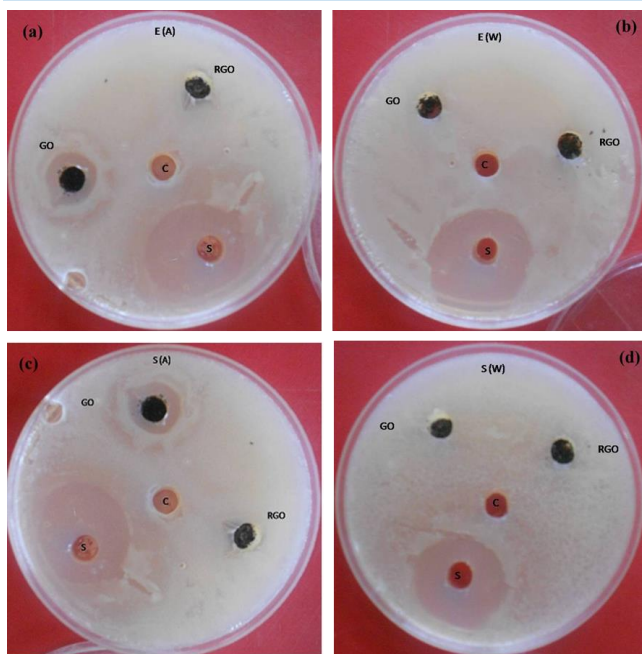


Fig. 7. Antibacterial effect of GO and RGO in comparison to streptomycin against *E. coli* in acetone (a), water (b) and against *S. aureus* in acetone (c), water (d).

Table 1. Antibacterial activity of GO, RGO and Streptomycin against bacterial pathogen *E. coli* and *S. Aureus* in water and acetone.

S. No.	Samples	Zone of Inhibition (mm) <i>E.coli</i>		Zone of Inhibition (mm) <i>S. aureus</i>	
		Water	Acetone	Water	Acetone
1.	GO	13	16	13	16.3
2.	RGO	11	12.3	09	10
3.	Streptomycin (S)	24	20	23	21
4.	Control (C)	No Zone	No Zone	No Zone	No Zone

Conclusion


Reduced graphite oxide (RGO) was prepared successfully as confirmed by SEM micrographs. The conversion of GO to RGO was seen through Raman as well as XRD spectra. The re-establishment of carbon sp^2 networks in RGO was also recognized by Raman spectra and was well supported by SEM images. Increase in UV absorption wavelength in comparison to GO also signifies the increase in conjugation leading to increase in sp^2 network bonded RGO. Thus it was concluded that chemical reduction is an effective method for the synthesis of RGO. High electrical conductivity of 1.363×10^4 S/m was recorded for RGO making it suitable for micro and nano electronic devices. Both GO and RGO showed good bactericidal effect against *Escherichia coli* and *Staphylococcus aureus*. Due to good bactericidal effects and high surface area, both GO and RGO can be further modified to form complexes usable in various biomedical applications including targeted drug delivery.

Reference

- Falkovsky, L. A. *J. Phys.: Conf. Ser.* **2008**, *129*, 012004. DOI: [10.1088/1742-6596/129/1/012004](https://doi.org/10.1088/1742-6596/129/1/012004)
- Lee, C.; Wei, X.; Kysar, J. W.; Hone, J. *Science* **2008**, *321*, 385. DOI: [10.1126/science.1156211](https://doi.org/10.1126/science.1156211)
- Balandin, A. A.; Ghosh, S.; Bao, W.; Calizo, I.; Teweldebrhan, D.; Miao, F.; Lau, C. N. *Nano Lett.* **2008**, *8*, 902. DOI: [10.1021/nl7031872](https://doi.org/10.1021/nl7031872)

- Ghosh, S.; Nika, D. L.; Pokatilov, E. P.; Balandin, A. A. *N. J. Phys.* **2009**, *11*, 095012. DOI: [10.1088/1367-2630/11/9/095012](https://doi.org/10.1088/1367-2630/11/9/095012)
- Tiwari, S. K.; Kumar, V.; Huczko, A.; Oraon, R.; Adhikari, A. D.; Nayak, G. C. *Crit. Rev. Solid State Mater. Sci.*, **2016**, *0*, 61. DOI: [10.1080/10408436.2015.1127206](https://doi.org/10.1080/10408436.2015.1127206)
- A. De Adhikari, R. Oraon, S. K. Tiwari, J. H. Lee, and G. C. Nayak, *RSC Adv.* **2015**, *5*, 27355. DOI: [10.1039/C4RA16174B](https://doi.org/10.1039/C4RA16174B)
- Parlak, O.; Beyazit, S.; Tse-Sum-Bui, B.; Haupt, K.; Turner, A. P. F.; Tiwari, A. *Nanoscale*, **2016**, *8*, 9976. DOI: [10.1039/C6NR02355J](https://doi.org/10.1039/C6NR02355J)
- Parlak O., Turnera A. P. F., Tiwari A. *J. Mater. Chem. B*, **2015**, *3*, 7434. DOI: [10.1039/C5TB01355K](https://doi.org/10.1039/C5TB01355K)
- Chen, J.; Peng, H.; Wang, X.; Shao, F.; Yuan, Z.; Han, H. *Nanoscale.*, **2014**, *6*, 1879. DOI: [10.1039/c3nr04941h](https://doi.org/10.1039/c3nr04941h)
- Liu, S.; Zeng, T. H.; Hofmann, M.; Burcombe, E.; Wei, J.; Jiang, R.; Kong, J.; Chen, Y. *ACS Nano.*, **2011**, *5*, 6971. DOI: [10.1021/nn202451x](https://doi.org/10.1021/nn202451x)
- Novoselov, K. S.; Geim, A. K.; Morozov, S. V.; Jiang, D.; Zhang, Y.; Dubonos, S. V.; Grigorieva, I. V.; Firsov, A. A. *Science.*, **2004**, *306*, 666. DOI: [10.1126/science.1102896](https://doi.org/10.1126/science.1102896)
- Hernandez, Y.; Nicolosi, V.; Lotya, M.; Blighe, F. M.; Sun, Z.; De, S.; McGovern, I. T.; Holland, B.; Byrne, M.; Gun'ko, Y. K.; Boland, J. J.; Niraj, P.; Duesberg, G.; Krishnamurty, S.; Goodhue, R.; Hutchison, J.; Scardaci, V.; Ferrari, A. C.; and Coleman, J. N. *Nat. Nanotechnol.*, **2008**, *3*, 563. DOI: [10.1038/nnano.2008.215](https://doi.org/10.1038/nnano.2008.215)
- Zhang, Y.; Gomez, L.; Ishikawa, F. N.; Madaria, A.; Ryu, K.; Wang, C.; Badmaev, A.; Zhou, C. W. Comparison of Graphene Growth on Single-Crystalline and Polycrystalline Ni by Chemical Vapor Deposition, *J. Phys. Chem. Lett.*, **2010**, *1*, 3101. DOI: [10.1021/jz1011466](https://doi.org/10.1021/jz1011466)
- Sutter, P. W.; Flege, J. I.; Sutter, E. A. *Nat. Mater.*, **2008**, *7*, 406. DOI: [10.1038/nmat2166](https://doi.org/10.1038/nmat2166)
- Thakur, A.; Kumar, S.; Rangra, V. S; *AIP Conf. Proc.*, **2015**, *1661*, 080032. DOI: [10.1063/1.4915423](https://doi.org/10.1063/1.4915423)
- Pei, S.; Cheng, H. M; *Carbon*, **2012**, *50*, 3210. DOI: [10.1016/j.carbon.2011.11.010](https://doi.org/10.1016/j.carbon.2011.11.010)
- Stankovich, S.; Dikin, D. A.; Dommett, G. H. B.; Kohlhaas, K. M.; Zimney, E. J.; Stach, E. A.; Piner, R. D.; Nguyen, S. T.; Ruoff, R. S; *Nature*, **2006**, *442*, 282. DOI: [10.1038/nature04969](https://doi.org/10.1038/nature04969)
- Kant, S.; Kumar, S; *J. Chem. Eng. Data.*, **2013**, *58*, 1294. DOI: [10.1021/je301362j](https://doi.org/10.1021/je301362j)
- Kant, S.; Kumar A.; Kumar, S; *J. Mol. Liq.*, **2009**, *150*, 39. DOI: [10.1016/j.molliq.2009.09.010](https://doi.org/10.1016/j.molliq.2009.09.010)
- Kumar, S.; Thakur, A.; Rangra, V. S.; Sharma, S; *Arab. J. Sci. Eng.*, **2016**, *41*, 2393. DOI: [10.1007/s13369-015-1852-1](https://doi.org/10.1007/s13369-015-1852-1)
- Ban, F. Y.; Majid, S. R.; Huang, N. M.; Lim, H. N; *Int. J. Electrochem. Sci.*, **2012**, *7*, 4345. ISSN [1452-3981](https://doi.org/10.1016/j.ultsonch.2012.09.007)
- Krishnamoorthy, K.; Kim, G-S; Kim, S. J; *Ultrason. Sonochem.*, **2013**, *20*, 644. DOI: [10.1016/j.ultsonch.2012.09.007](https://doi.org/10.1016/j.ultsonch.2012.09.007)
- Wang, G.; Shen, X.; Wang, B.; Yao, J.; Park; *J. Carbon.*, **2009**, *47*, 1359. DOI: [10.1016/j.carbon.2009.01.027](https://doi.org/10.1016/j.carbon.2009.01.027)
- Park, S.; An, J.; Potts, J. R.; Velamakanni, A.; Murali, S.; Ruoff, R. *Carbon.*, **2011**, *49*, 3019. DOI: [10.1016/j.carbon.2011.02.071](https://doi.org/10.1016/j.carbon.2011.02.071)
- Bykkam, S.; Venkateswara, R.K., Shilpa Chakra CH.; Thunugunta, T; *Int. J. of Adv. Biotech. and Research*, **2013**, *4*, 142. ISSN [0976-2612](https://doi.org/10.1016/j.ultsonch.2012.09.007).
- Some, S.; Kim, Y.; Yoon, Y.; Yoo, H.; Lee, S.; Park Y.; Lee, H; *Sci. Rep.*, **2013**, *3*, 1929. DOI: [10.1038/srep01929](https://doi.org/10.1038/srep01929)
- Subrahmanyam, K. S.; Vivekchand, S. R. C.; Govindaraj, A.; Rao, C. N. R; *J. Mater. Chem.*, **2008**, *18*, 1517. DOI: [10.1039/B716536F](https://doi.org/10.1039/B716536F)
- Li, X.; Zhang, G.; Bai, X.; Sun, X.; Wang, X.; Wang, E.; Dai, H; *Nat. Nanotechnol.*, **2008**, *3*, 538. DOI: [10.1038/nnano.2008.210](https://doi.org/10.1038/nnano.2008.210)

29. Cao, A. N.; Liu, Z.; Chu, S. S.; Wu, M. H.; Ye, Z. M.; Cai, Z. W.; Chang, Y. L.; Wang, S. F.; Gong, Q. H.; Liu, Y. F; *Adv. Mater.* **2010**, *22*, 103.
DOI: [10.1002/adma.200901920](https://doi.org/10.1002/adma.200901920)
30. Ferrari, A. C.; Robertson, J; *Phys. Rev. B.*, **2001**, *64*, 075141.
DOI: [10.1103/PhysRevB.64.075414](https://doi.org/10.1103/PhysRevB.64.075414)
31. Thomsen, C.; Reich, S; *Phys. Rev. Lett.*, **2000**, *85*, 5214.
DOI: [10.1103/PhysRevLett.85.5214](https://doi.org/10.1103/PhysRevLett.85.5214)
32. Casiraghi, C.; Hartschuh, A.; Qian, H.; Piscanec, S.; Georgi, C.; Fasoli, A.; Novoselov, K. S.; Basko, D. M.; Ferrari, A. C; *Nano Lett.*, **2009**, *9*, 1433.
DOI: [10.1021/nl8032697](https://doi.org/10.1021/nl8032697)
33. Kuila, T.; Khanra, P.; Bose, S.; Kim, N. H.; Ku, B. C.; Moon B.; Lee, J. H; *IOP Nanotechnol.*, **2011**, *22*, 305710.
DOI: [10.1088/0957-4484/22/30/305710](https://doi.org/10.1088/0957-4484/22/30/305710)
34. Pimenta, M. A.; Dresselhaus, G.; Dresselhaus, M. S.; Cancado, L. G.; Jorio, A.; Saito, R; *Phys. Chem. Chem. Phys.*, **2007**, *9*, 1276.
DOI: [10.1039/B613962K](https://doi.org/10.1039/B613962K)
35. Srinivas, G.; Zhu, Y.; Piner, R.; Skipper, N.; Ellerby, M.; Ruoff, R; *Carbon*. **2010**, *48*, 630.
DOI: [10.1016/j.carbon.2009.10.003](https://doi.org/10.1016/j.carbon.2009.10.003)
36. Fu, C.; Zhao, G.; Zhang, H.; Li, S; *Int. J. Electrochem. Sci.*, **2013**, *8*, 6269.
37. Chuang, C.H.; Wang, Y.F.; Shao, Y.C.; Yeh, Y.C.; Wang, D.-Y.; Chen, C.-W.; Chiou, J. W.; Ray, S. C.; Pong, W. F.; Zhang, L.; Zhu J.F.; Guo, J. H; *Sci. Rep.*, **2014**, *4*, 4525.
DOI: [10.1038/srep04525](https://doi.org/10.1038/srep04525)
38. Thema, F. T.; Moloto, M. J.; Dikio, E. D.; Nyangiwe, N. N.; Kotsedi, L.; Maaza, M.; Khenfouch, M; *J. of Chem.*, **2013**, *2013*, 150536.
DOI: [10.1155/2013/150536](https://doi.org/10.1155/2013/150536)
39. Loryuenyong, V.; Totepvimarn, K.; Eimburanaprat, P.; Boonchompoo, W.; Buasri, A. *Adv. Mater. Sci. Eng.* **2013**, *2013*, 923403.
DOI: [10.1155/2013/923403](https://doi.org/10.1155/2013/923403)
40. Akihiko, K.; Ryo, N.; Akihide, I.; Hideki, K. *Chem. Phys.* **2007**, *339*, 104.
DOI: [10.1016/j.chemphys.2007.07.024](https://doi.org/10.1016/j.chemphys.2007.07.024)
41. Liu, Z.; Robinson, J. T.; Sun, X.; Dai, H. *J. Am. Chem. Soc.* **2008**, *130*, 10876.
DOI: [10.1021/ja803688x](https://doi.org/10.1021/ja803688x)
42. Luo, Z.; Vora, P. M.; Mele, E. J.; Johnson, A. T. C.; Kikkawa, J. M. *Appl. Phys. Lett.* **2009**, *94*, 111909.
DOI: [10.1063/1.3098358](https://doi.org/10.1063/1.3098358)
43. Geng, Y.; Wang, S. J.; Kim, J. K; *J. of Colloid and Interface Sci.* **2009**, *336*, 592.
DOI: [10.1016/j.jcis.2009.04.005](https://doi.org/10.1016/j.jcis.2009.04.005)
44. Shan, C.; Yang, H.; Han, D.; Zhang, Q.; Ivaska, A.; Niu, L; *Langmuir*, **2009**, *25*, 12030.
DOI: [10.1021/la903265p](https://doi.org/10.1021/la903265p)



A Monthly Journal

Advanced Materials Letters

Volume 7, December 2016

An official journal of International Association of Advanced Materials
www.iaamonline.org


Available online at
www.vbripress.com

Copyright © 2016 VBRI Press AB, Sweden

Publish your article in this journal

Advanced Materials Letters is an official international journal of International Association of Advanced Materials (IAAM, www.iaamonline.org) published monthly by VBRI Press AB from Sweden. The journal is intended to provide high-quality peer-review articles in the fascinating field of materials science and technology particularly in the area of structure, synthesis and processing, characterisation, advanced-state properties and applications of materials. All published articles are indexed in various databases and are available download for free. The manuscript management system is completely electronic and has fast and fair peer-review process. The journal includes review article, research article, notes, letter to editor and short communications.

www.vbripress.com/aml



VBRI Press
Commitment to Excellence